Journal of Thermal Analysis and Calorimetry, Vol. 71 (2003) 249–261

STUDY OF α- AND β-RELAXATION PROCESSES IN SUPERCOOLED SUCROSE LIQUIDS

D. Champion[1*], *M. Maglione*[2], *G. Niquet*[3], *D. Simatos*[1] *and M. Le Meste*[1]

[1]Laboratoire d'Ingénierie Moléculaire et Sensorielle de l'Aliment, ENSBANA, Université de Bourgogne, 21000 Dijon, France
[2]Institut de Chimie de la Matière Condensée de Bordeaux, CNRS, 33608 Pessac Cedex, France
[3]Laboratoire de microélectronique, Bâtiment Gabriel. Université de Bourgogne, 21000 Dijon, France

Abstract

The relaxation map of highly concentrated sucrose water mixtures was built using mechanical and impedance spectroscopies. Data of α- and β-relaxation processes obtained with both techniques complete calorimetric and rheological measurements. The temperature evolutions of the relaxations were extrapolated using the measured data and the equations commonly used to describe the relaxations: Arrhenius and WLF behaviours for respectively the β- and α-relaxations. The temperature/frequency domain when α and β processes merge for 99% sucrose solution is discussed with respect to scenery proposed in the literature.

Keywords: α- and β-relaxations, dielectric spectroscopy (DS), dynamic mechanical spectroscopy (DMS), glass transition, sucrose

Introduction

Sugars (glucose, sucrose, maltose...) are the main constituents of many foods and pharmaceutical preparations. They are used for their sweetness or protective properties, but also as matrices where other molecules are entrapped (active components for drugs, aroma for glassy sweets...). The loss of quality of these low moisture products during storage is mainly controlled by the mobility of the reacting species within the matrix, by the release of aroma compounds due to diffusion as related to the mobility of constitutive molecules involved in collapse or crystallization. Several studies concerning the influence of the physical state of the matrix on the molecular mobility have been reported. On the one hand the diffusion coefficients of the exogenous molecules (volatile compounds [1, 2] or probes [3, 4]) dispersed in the matrix were measured and on the other hand the relaxation phenomena within the matrix were studied to identify the parameters controlling molecular mobility.

* Author for correspondence: E-mail: dchamp@u-bourgogne.fr

1418–2874/2003/ $ 20.00
Akadémiai Kiadó, Budapest

Two different relaxation phenomena have been reported in small carbohydrate matrices such as glucose [5, 6], maltose [7], galactose, sorbitol [8–10], so called: the α- and β-relaxations. The α- (main or primary) relaxation has been associated to the glass transition and to subsequent changes in the matrix viscosity. It corresponds to highly cooperative global motions (translational) of the matrix molecules. The β- (or secondary) relaxations (as described by Johari) correspond to more localised molecular motions which persist in the glassy state [6]. In carbohydrate, the β process, often detected using dielectric spectroscopy (DS), was initially associated to OH groups motions. More recently, it has been demonstrated that this relaxation is sensitive to the molecular structure of the carbohydrate and could be due to the rotation of the whole molecules in matrix defects [11].

The kinetic glass transition concept associated to the primary relaxation phenomenon has been widely used to delineate molecular mobility as a function of temperature and composition. However several studies have recently demonstrated that T_g, an operationally defined glass transition temperature, cannot be used as a threshold reference temperature for small molecule mobility in glass-forming liquid [12] when the radius of the diffusing molecule is in the same order of magnitude as the matrix constitutive molecules [13]. Moreover, it has been shown that the secondary relaxation process may facilitate the diffusion of a small molecule such as fluorescein in the vicinity of the glass transition of concentrated sucrose solutions [4].

The main objectives of this work are (i) to study the β-relaxation in supercooled concentrated sucrose solutions using DS measurements and (ii) to study the crossover between α- and β-relaxation processes using both mechanical and impedance spectroscopy data. Impedance spectroscopy was performed to study the secondary relaxation in vitreous sucrose solution because these samples were too brittle and rigid to be analysed by mechanical spectroscopy. Data for α- and β-relaxation processes obtained with both techniques supplement calorimetric and rheological measurements of the sucrose water mixtures. All results were analysed in this paper according to different theoretical formalisms describing the relaxation processes with respect to the temperature dependence of their characteristic relaxation time (τ_{mol}).

Material and methods

Sample preparation

Sucrose solutions from 84 to 90% (*w*/*w*) were prepared by dehydration of a 50% sucrose solution at a temperature lower than 140°C. Concentration was performed under vigorous agitation in a temperature-controlled oil bath. The water content of the sample was determined from the mass loss. The viscous sucrose water mixtures were subsequently poured into cells adapted to each measuring techniques:

• Dynamic mechanical spectroscopy: a cylindrical mould (16 mm high×6 mm i.d.) was used for 90 to 98% solutions in order to perform a tension-compression tests while hot solutions (82%) were introduced between the annular shear holders (10 mm annular diameter and 8 mm piston rod) for annular shear tests.

- Dielectric spectroscopy: the cell consisted in 2 metal electrodes (28 mm^2 surface) on the bottom and the top separated by a 1–2 mm thick Teflon spacer. The rapid decrease in temperature allowed the glass formation from the viscous liquid without any sucrose crystallisation.

Dynamic mechanical spectroscopy

A viscoanalyser (Metravib RDS, France) was used to apply two different harmonic excitation modes: tension-compression tests with strain amplitude of $3 \cdot 10^{-6}$ m or annular shear tests with strain amplitude at $5 \cdot 10^{-6}$ m. All measurements were carried out in the linear range of viscoelasticity i.e below $10 \cdot 10^{-6}$ m maximum strain at 40 Hz. For the tension-compression tests, the glassy sucrose solid was extracted from the mould, glued (Duratrode Super SP, Amatron, France or 1-X60, HBM, Germany) onto the sample holders and covered with silicon grease (Silbione Pâte 70428, Rhone Poulenc, France) to prevent as far as possible dehydration during the analysis. For annular shearing tests, mineral oil for microscopy (Nachet, France) was layered on top of the sample before cooling. The temperature within the furnace was monitored to ±1°C with a Pt100 probe located at 4 mm from the sample. The measurement of the stiffness and of the loss angle δ allowed the calculation of the viscoelastic parameters: i.e. the storage (E' or G') and loss components (E'' or G'') of the dynamic moduli E^* or G^* and the loss angle tangent. All measurements were carried out at 4 different excitation frequencies from 5 to 50 Hz solicitations during heating ramp 2 K min^{-1} following a precooling rate at 2 K min^{-1}.

Dielectric spectroscopy

Dielectric complex and loss angle were measured with an HP 4284A LCR meter (Hewlett Packard, France). Temperature was controlled by a Lake Shore DRC93 regulation, with a temperature probe located at 3 mm to the bottom electrode; the temperature was monitored ±0.1°C. Measurements of the real and imaginary component of dielectric permittivity, ε′ and ε″, were made at 21 frequencies in the range 1 to 1000 kHz, during a temperature upscan at 0.5 K min^{-1}. Frequency sweeps were also performed at 59 frequencies from 1 to 1000 kHz in purely isothermal conditions in order to confirm the result from the previous hybrid protocols.

Mechanical and dielectric measurements were repeated at least three times but it was not possible to obtain exactly the same water content for each replicate, so instead of considering the mean for the different measurements, each replicate was taken into account individually in the composition of the relaxation map (no standard deviations were calculated). The accuracy of the water content determination was around 1%.

DSC measurement

A Perkin Elmer DSC7 calorimeter was used at 10 K min^{-1} to measure heat capacity and glass transition temperature (T_g) of the sucrose preparations. The DSC was calibrated with pure azobenzol (T_m=68°C) and indium (T_m=156.7°C). Two heating pro-

grams were applied. The first one allowed to determine the calorimetric glass transition temperature range when heating at 10 K min^{-1} and to completely melt the sample at a temperature lower than 195°C (this avoids sugar degradation [14]). A second scan was applied to precisely determine the value of T_g and measure the temperature difference between the onset and end temperatures of the glass transition in order to control sample integrity. The transition spans over a wider temperature range when sucrose hydrolysis occurs. With DSC, we could also control that negligible dehydration took place during spectroscopic assays if identical traces on thermograms were obtained before and after experiments. The considered values of T_g in this work for calculations were for the onset of the glass transition.

Viscosity measurement

The viscosity of sucrose solutions was measured with a rheometer (Rh 30, Contraves). A Couette geometry was used with a 4 mm gap between the cup (80 mL) and inner cylinder. The deformation rate varied between 0 and 100 s^{-1}. The viscosity was monitored as a function of temperature for a 65.3% (*w*/*w*) sucrose solution, i.e. from 20 to –15±1°C.

Results and discussion

The effect of water content on the calorimetric glass transition temperature at 10 K min^{-1} of sucrose-water mixtures (T_g) was taken into account using the Gordon Taylor equation taken with T_g onset for dry sucrose and water as 338 and 135 K [15] respectively and coefficient k=5.46 as determined from the data published by Blond *et al*. [16].

In the temperature range considered, between T_g and T_g +100°C, the viscosity is linked to T_g according to the WLF equation [17]:

$$\log(\eta_T / \eta_{T_g}) = C_{g1}(T - T_g)/(C_{g2} + T - T_g) \quad (1)$$

with C_{g1} and C_{g2} the WLF coefficients determined for sucrose solutions, respectively 19.8 and 51.6 K [4] and η_T, η_{T_g} the viscosity (Pa.s) at the temperature T and T_g respectively ($\eta_{T_g} = 1.6 \cdot 10^{12}$ Pa.s, calculated using T_g onset for the glass transition temperature). The viscosity of 65.3% (*w*/*w*) sucrose solutions was measured in the temperature range corresponding to the WLF domain (T_g, T_g+100) and only for samples not containing ice crystals; that is down to –15°C [15]. Our measurement set-up did not allow us to carry out viscosity measurements without sucrose crystallisation, for low water content solutions, i.e. for sucrose concentration higher than 70%.

From the equations describing the rheological properties of highly viscous liquids developed by Maxwell–Kelvin–Voigt, the characteristic relaxation time (τ_η) is connected to the viscosity (η) by:

$$\tau_\eta = \eta / G_\infty \quad (2)$$

G_∞ the complex modulus (Pa) at infinite frequency; the value is about $2 \cdot 10^9$ Pa and changes only slightly (from 2 to $4 \cdot 10^9$ Pa) [18]from one substance to another [19].

In DMS studies, a decrease of the storage modulus (E' or G') and a peak in the loss modulus (E'' or G''), at a temperature depending on the excitation frequency, are characteristic of a relaxation phenomenon. Figure 1 shows the evolution of these viscoelasticity parameters E', E'' and $\tan\delta=E''/E'$ measured in a quasi-isothermal tension-compression test at 5 Hz for a 93% sucrose solution during a heating ramp at 2 K min^{-1}. At low temperatures, the sample was glassy: the storage modulus E' was 10^9 Pa and did not evolve a lot with temperature. E'' was also high but lower than E' as expected for a solid sample. The influence of the primary relaxation (Fig. 1) induced a sharp decrease in E' and a peak in E'' due to a maximum of dissipated energy at a frequency characteristic of major thermally activated molecule friction. The loss modulus became higher than the E' value after the relaxation because the sample was a viscous liquid. Tanδ for a small solute solution should not show a maximum but in our experiment, the onset of the sample flow made the measurements unreliable at higher temperature (T>20°C). The same evolution of G' and G'' were observed in annular shear test (data not shown).

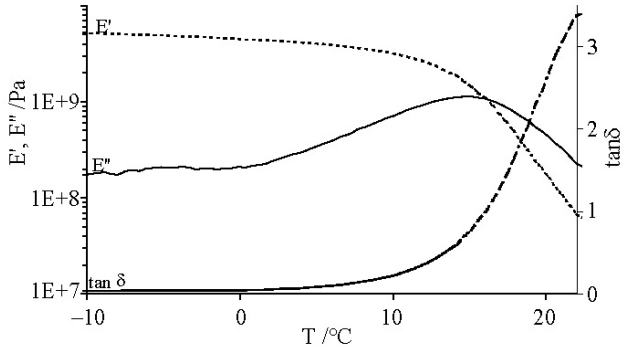

Fig. 1 Isochronous (5 Hz) tension-compression dynamical testing of 93% sucrose solution heated at a 2 K min^{-1}. E', E'' are the conservative and dissipative moduli and $\tan\delta=E''/E'$ the loss factor

Isothermal experiments over a wide frequency range offer an alternative approach to observe more rigorously the mechanical relaxations. However, the results obtained by strictly or quasi-isothermal assays were comparable for samples of identical water content. The influence of frequency on the relaxation phenomena from –10 to 25°C is presented on Fig. 2. The maximum of E'' was shifted to higher temperature with an increase of frequency. E'' showed a small peak at lower temperatures which could not be analysed due to the low amplitude of the phenomenon, but it was assumed to be the sign of a secondary relaxation.

Considering linear viscoelasticity theory and assuming that $\omega\tau_{mol}=1$ when $G''_{(\omega)}$ is maximum, the characteristic relaxation time (τ_{mol}) of the sucrose molecule is deduced for resonance conditions:

$$\tau_{mol}=1/2\pi F \quad (3)$$

where F is the measurement frequency in Hz ($F=\omega/2\pi$, with ω the angular velocity).

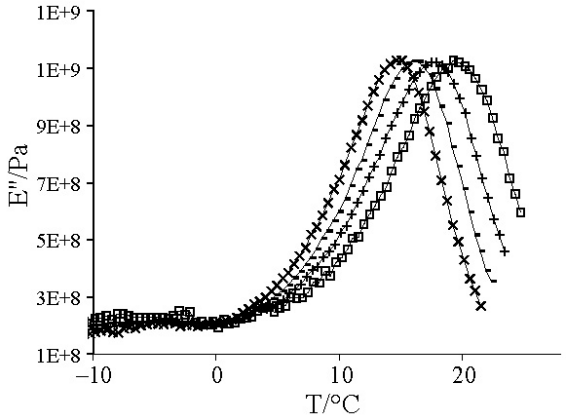

Fig. 2 Frequency dependence of isochronous loss modulus in condition similar to Fig. × – 1; 5 Hz, — – 10 Hz, + – 20 Hz and □ – 50 Hz

Annular shearing tests were also used to study 82 and 80% sucrose solutions with DMS. Dynamic viscosity η^* was calculated using recorded data for G' and G'' at different frequencies:

$$\left|\eta^*\right| = \sqrt{G'^2 + G''^2}/2\pi F \tag{4}$$

According to the Cox–Merz rule [20], which states that the (steady state) viscosity *vs.* shear rate curve is virtually identical to the dynamic viscosity *vs.* frequency curve, the relaxation time obtained from experimental dynamic viscosity values was calculated with Eq. (2) and presented in Fig. 3.

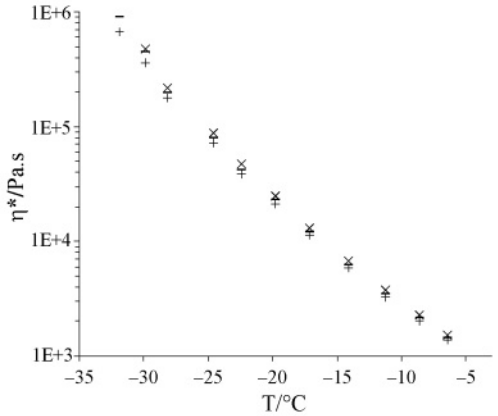

Fig. 3 Dynamic viscosity η^* of a 80% sucrose solution measured at different frequencies × – 5 Hz, — – 10 Hz, + – 20 Hz *vs*. temperature (annular shear test)

For more concentrated sucrose solution (99% *w*/*w*), Fig. 4 shows the evolution of the dielectric loss component (ε″) as a function of frequency at different temperatures from –31 to –5°C. In a similar way to mechanical spectroscopy, the reference

temperature for relaxation was taken as the temperature of ε″ max and the characteristic relaxation times were calculated with Eq. (3). The amplitude of the ε″ peaks increased significantly when the temperature was increased. A similar evolution has been reported for sorbitol above its calorimetric T_g but the interpretation of this phenomenon has not yet been elucidated [18].

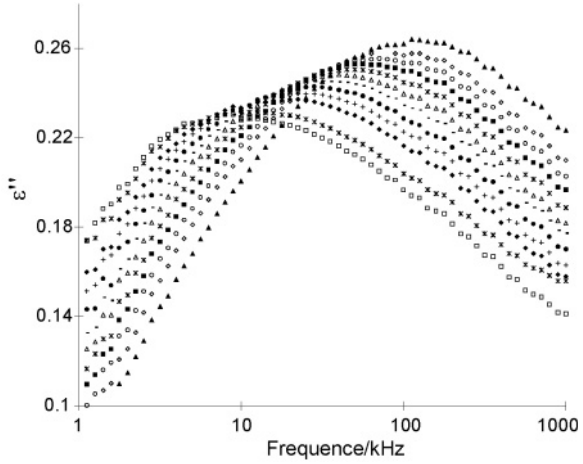

Fig. 4 Series of isothermal dielectric loss component ε″ spectra in the β-relaxation range *vs*. temperatures from □ – –31°C to ▲ – –5°C by 2°C step for a 99% sucrose solution

From the frequency shift at peak maximum E'' (or ε″) with reciprocal temperature, an Arrhenius analysis of thermally activated processes may be applied (Figs 2 and 4). The kinetic aspect of the relaxations is demonstrated by this frequency dependence property; while melting (or crystallisation) would not show such behaviour. The apparent activation energy (E_a) of the relaxation can be calculated from the relation:

$$\ln F = -E_a/RT + A \quad (4)$$

F is the frequency (Hz), T the temperature (K) of the maximum of ε″ or E'', R the gas constant and A is a constant.

Whatever the relaxation, Eq. (4) may be used to calculate an apparent activation energy and this value allows the discrimination between primary or secondary relaxations. For a β-relaxation, E_a can be calculated over a relatively extended range of temperatures due to the rather strict Arrhenius behaviour (Fig. 5). On the contrary, for an α process, E_a has to be approximated over a restricted temperature range [9]. Moreover, the closer to T_g (but above), the higher is the activation energy due to the WLF behaviour of the primary relaxation. Table 1 shows such apparent activation energies of the relaxations processes observed with by DS and DMS. ($T_{gDSC}/T_{\alpha(5\ Hz)}$) is the normalizing ratio which scales the primary relaxation data (with T_g the onset temperature of glass transition obtained by DSC at 10 K min^{-1} and $T_{\alpha(5\ Hz)}$ the temperature of E'' maximum at 5 Hz). E_a depends on the size of the relaxing entity [8] and the cooperative character of the relaxation [21]. As expected, local motions of more independent β processes yield lower activation energies.

Typical literature values for sugars (maltose or glucose) are found between 40 and 70 kJ mol^{-1} for β-relaxation processes, while for cooperative α-relaxation values vary from 200 to 400 kJ mol^{-1} close to calorimetric T_g [6, 7]. Our data for sucrose agree with such an order of magnitude (Table 1).

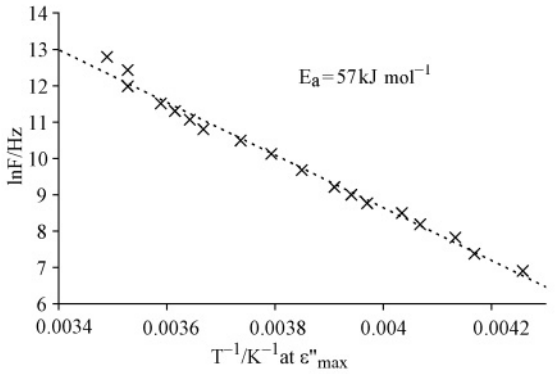

Fig. 5 Arrhenius plot of the dielectric loss peak frequency *vs*. the reciprocal temperature for a 99% sucrose solution

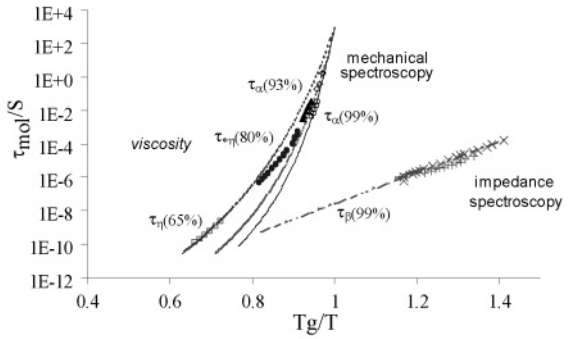

Fig. 6 Composite relaxation map of concentrated sucrose melts. Characteristic relaxation times (τ_{mol} in s) deduced from different techniques: o – α-relaxation time (τ_α) obtained by DMS for a 99% sucrose solution, △ – and ▲ – τ_α by DMS for 93% (data are quasi superposed), ◇ – measurements done in isothermal conditions at 10^{-1} Hz, ● – τ_η. issued from complex viscosity for 80%, +, – and × – τ_β by DS for 99% sucrose solutions, □ – τ_η from viscosity measurements for 65% sucrose. The continuous lines for the α-relaxation of 99, 93 and 65% sucrose solutions were obtained by calculation using WLF equation (with C_{g1}=–19.8 and C_{g2}=51.6 K [4])

In order to gather our results obtained with the different techniques, molecular mobility has been expressed through of characteristic relaxation times (τ_{mol}) as deduced from Eq. (3) for spectroscopic techniques (DMS and DS) and from Eq. (2) for rheological measurements. The mobility map of the different sucrose-water mixtures shows the relaxation times variations *vs.* the reciprocal temperature normalized to T_g (Fig. 6). The in-

Table 1 Apparent activation energies calculated from dielectric (for β-relaxation) or mechanical (for α-relaxation) spectroscopy data (the accuracy of the determination of water content was ±1%)

Sucrose/%	$T_{gDSC}/T_{\alpha(5\ Hz)}$	E_a/kJ mol^{-1}		onset T_g/K
		dielectric spectroscopy	mechanical spectroscopy	
82	0.96		281	227
93	0.94		276	279
93	0.98		350	279
96	0.99		374	300
99	0.96		395	327
98	Arrhenius behaviour	62		318
99	Arrhenius behaviour	61		327
99	Arrhenius behaviour	57		327

fluence of hydration is thus partially accounted for as T_g depends on plasticizer content. Such a plot is similar to the representation proposed by Angell [22] to classify glass forming liquids according to the influence of temperature on τ_α above glass transition temperature. The fragility parameter *m* was introduced to differentiate fragile systems (*m* between 100 and 200) which show a sharp decrease of τ_α in the vicinity of T_g, from strong ones (*m* between 16 and 100) which evolve with quasi Arrhenian behaviour. By definition, *m* is the slope of the scaled Arrhenius plot of viscosity when temperature approaches T_g from above:

$$m=E_a/(\lg RT_g) \quad (5)$$

Equation (5) was used to calculate fragility parameters *m* as a function of water content in the sample with apparent activation energies reported in Table 1. The value obtained varied between 52 and 65 independently on the concentration of the melt. Since the ratio $T_{gDSC}/T_{\alpha(5\ Hz)}$ were different, the slope which had been taken into account for E_a determination might not reflect the fragility but was function of the distance from T_g.

As a first order approximation in this work, the effect of water content on fragility (*m*) of the sucrose solutions close to T_g was neglected. Actually, τ_α data sets for all water contents were fitted using the same WLF coefficients (with C_{g1}=–19.8 and C_{g2}=51.6 K [4]) which implies that the effect of plasticization was solely introduced through the dependence of T_g value on hydration used in WLF equation (continuous lines in Fig. 6).

Thanks to the overlapping time scales of the combined techniques, data for both primary and secondary relaxation may be presented. Due to the large difference in apparent activation energies, the WLF behaving α-relaxation and the Arrhenian β-relaxation are expected to overlap at $T_{\alpha\beta}$, the crossover temperature, where maximal dissipative frequencies turn to be equal. $T_{\alpha\beta}$ seems to occur for several glass forming liquids with typical uncertainties of about 10 K for the temperature and more than one decade for the frequency domain whatever the technique used for the determination of relaxation times [23]. Indeed, the characteristic relaxation time values at the merging temperature ($\tau_{\alpha\beta}$) has been given for several glass-forming liquids in a typical range from 10^{-6} to 10^{-8} s [24]. However, the mobility map, given by the same author [25], for polybutadiene and obtained by neutron scattering and NMR techniques, shows an αβ merging region with a relaxation time around 10^{-9} s. Beiner and collaborators [23] reported a large literature data collection. They showed that $\tau_{\alpha\beta}$ may vary from as much as 10^{-2} to 10^{-10} s for polymers and small molecules glass formers, but most systems belong to the 10^{-6} to 10^{-8} s range for $\tau_{\alpha\beta}$. In our case, the crossover temperature was determined by calculation with the extrapolation of the Arrhenius law for the β process and with the WLF prediction of the relaxation time for viscosity (Fig. 6). In fact, only the 99% melt allowed a legitimate extrapolation of τ_β dielectric and τ_α mechanical leading to order of magnitude of $\tau_{\alpha\beta}\approx10^{-10}$ s and $T_{\alpha\beta}\approx1.2T_g$.

Some values reported for glycerol: $\tau_{\alpha\beta}\approx3\cdot10^{-9}$ s and $T_{\alpha\beta}\approx1.39T_g$ [23] and sorbitol: $\tau_{\alpha\beta}\approx10^{-7}$ s and $T_{\alpha\beta}\approx1.1T_g$ [9] are in reasonable agreement with our finding. Yet the rather low value for $T_{\alpha\beta}$ might be attributed to the extrapolation of dielectric permittivity data. Our value for $\tau_{\alpha\beta}$ is low compared with those of literature but it is known that the data ob-

tained from impedance spectroscopy might give slightly lower relaxation times (up to 1 decade) compared with relaxation times obtained with other methods as calorimetry [26]. In the same way, relaxation times obtained in glucose/water solutions using dielectric spectroscopy and NMR differ in magnitude on 3 decades [5].

Below the merging $T_{\alpha\beta}$, both relaxation processes may be observed; while only one relaxation mode remains above, yet with a sustained WLF behaviour. At $T_{\alpha\beta}$, the dynamic behaviour and other physical properties change: i) an enhancement of translational diffusion compared to rotational diffusion [13, 27, 28] or compared to viscosity [29, 4] has been identified and, ii) a change of the WLF parameters from one parameter set to another one [23] was reported.

Conclusions

In order to establish the mobility map of sucrose solutions around the glass transition range, the combination of several techniques was necessary. However, the use of different methods to determine relaxation times raises methodological issues about the exploitation of the results, the comparison between them, and the precise definition of particular temperature such as $T_{\alpha\beta}$. Indeed, the measurements of relaxation times over a wide range of temperature induce the use of different types of excitations and because E_a are the same in temperature/frequency domain, the response is assigned to a similar relaxation phenomenon. However, depending on the nature of excitations (calorimetric, mechanical or dielectric), the value of τ can be different at the same frequency and linked to the solicitation.

Several theoretical equations were employed to approximate the evolution of α- and β-relaxation processes and thus, obtain an estimate of $T_{\alpha\beta}$. The temperature is of interest to understand the possible decoupling of translational diffusion from viscosity on Stokes–Einstein relation in the vicinity of T_g. However, the mobility map does not account for the distributed character of the relaxation times, which is a stringent specificity of cooperatively interacting systems above and below T_g.

* * *

This work has been carried out with financial support from the Commission of the European Communities, Agriculture and Fisheries (FAIR) specific RTD program, Contract CT-96-1085 'Enhancement of Quality of Food and Related Systems by Control of Molecular Mobility'. It does not necessary reflect its views and in no way anticipates the Commission's future policy in this area.

List of symbols

A	constant or pre-exponential factor
C_{g1}, C_{g2}	the WLF coefficients
DS	dielectric spectroscopy
DMS	dynamic mechanical spectroscopy
DSC	differential scanning calorimetry

E' and E''	real and imaginary values of the complex Young modulus E^*
ε' and ε''	real and imaginary values of the electric permittivity ε^*
E_a	apparent activation energy
F	Frequency (Hz)
G' and G''	real and imaginary values of the complex Coulomb modulus G^*
G_∞	the complex modulus (Pa) at infinite frequency
k	Gordon Taylor coefficient
m	fragility parameter
T	temperature (K)
T_m	melting temperature
T_g or T_{gDSC}	calorimetric glass transition temperature
$T_{\alpha\beta}$	α and β relaxation processes merging temperature
R	gas constant (8.314 J mol^{-1} K^{-1})
τ_{mol}	characteristic relaxation time (generic name)
τ_η	if deduced from steady state viscosity measurements (Eq. 2)
τ_{η^*}	if deduced from dynamic viscosity measurements
τ_α	for α-relaxation time obtained by DMS
τ_β	for β-relaxation time obtained by DMS
$\tau_{\alpha\beta}$	the characteristic relaxation time at temperature $T_{\alpha\beta}$
η_T	viscosity at temperature T
η^*	dynamic viscosity
WLF	Williams Landel Ferry
ω	the angular velocity

References

1 I. Goubet, J. L. Le Quere and A. Voilley, J. Agric. Chem., 46 (1998) 1981.
2 M. Rosenberg, I. J. Kopelman and Y. Talmon, J. Agric. Chem., 38 (1990) 1288.
3 R. Chakraborty and K. A. Berglund, AIChE Symp. Ser., 87 (1991) 114.
4 D. Champion, H. Hervet, G. Blond, M. Le Meste and D. Simatos, J. Phys. Chem. B, 10 (1997) 10674.
5 G. R. Moran, K. R. Jeffrey, J. M. Thomas and J. R. Stevens, Carb. Res., 328 (2000) 573.
6 R. K. Chan, K. Pathmanthan and G. P. Johari, J. Phys. Chem., 90 (1986) 6358.
7 T. R. Noel, R. Parker and S. G. Ring, Carb. Res., 282 (1996) 193.
8 Gangasharan and S. S. N. Murthy, J. Phys. Chem., 99 (1995) 12349.
9 R. Nozaki, D. Suzuki, S. Ozawa and Y. Shiozaki, J. Non-Cryst. Solids, 235–237 (1998) 393.
10 N. B. Olsen, J. Non-Cryst. Solids, 235–237 (1998) 399.
11 H. Wagner and R. Richert, J. Non-Cryst. Solids, 242 (1998) 19.
12 R. Parker and S. G. Ring, Carb. Res., 273 (1995) 147.
13 F. Fujara, B. Geil, H. Sillescu and G. Fleischer, Z. Phys. B. Cond. Matt., 88 (1992) 195.

14 I. Vanhal and G. Blond, J. Agric. Chem., 47 (1999) 4285.
15 C. A. Angell and J. C. Tucker, J. Phys. Chem., 84 (1980) 268.
16 G. Blond, D. Simatos, M. Catte, C. G. Dussap and J. B. Gros, Carb. Res., 298 (1997) 139.
17 M. L. Williams, R. F. Landel and J. D. Ferry, J. Am. Chem. Soc., 77 (1955) 3700.
18 A. Faivre, L. David and J. Perez, J. Phys II., 7 (1997) 1635.
19 P. B. McNulty and D. G. Flynn, Transactions of the ASAE, (1979) 445.
20 M. Renardy, J. Non-Newton, Fluid Mech., 68 (1997) 133.
21 E. Donth, Physica Scripta, T49 (1993) 223.
22 C. A. Angell, J. Phys. Chem. Solids, 49 (1988) 863.
23 M. Beiner, H. Huth and K. Schroter, J. Non-Cryst. Solids, 279 (2001) 126.
24 A. P. Sokolov, J. Non-Cryst. Solids, 235–237 (1998) 190.
25 E. Rossler and A. P. Sokolov, Chemical Geology, 128 (1996) 143.
26 J. E. K. Schawe, Thermochim. Acta, 388 (2002) 299.
27 E. Rössler, J. Tauchert and P. Eiermann, J. Phys. Chem., 98 (1994) 8173.
28 D. B. Hall, D. D. Deppe, K. E. Hamilton, A. Dhinojwala and J. M. Torkelson, J. Non-Cryst. Solids, 235–237 (1998) 48.
29 M. T. Cicerone, F. R. Blackburn and M. D. Ediger, J. Chem. Phys., 102 (1995) 471.